Mammalian Mechanoelectrical Transduction: Structure and Function of Force-Gated Ion Channels

Dominique Douguet, Eric Honoré

Mammalian mechanoelectrical transduction: structure and function of force-gated ion channels

Dominique Douguet and Eric Honoré*

Université Côte d'Azur, Centre National de la Recherche Scientifique, Institut national de la santé et de la recherche médicale, Institut de Pharmacologie Moléculaire et Cellulaire, Labex ICST, Valbonne, France.

*Corresponding author

The conversion of force into an electrical cellular signal is mediated by the opening of different types of mechanosensitive ion channels (MSCs), including TREK/TRAAK K_{2P} channels, Piezo1/2, TMEM63/OSCA and TMC1/2. Mechanoelectrical transduction plays a key role in hearing, balance, touch, proprioception and is also implicated in the autonomic regulation of blood pressure and breathing. Thus, dysfunction of MSCs is associated with a variety of inherited and acquired disease states. Significant progress has recently been made in identifying these channels, solving their structure and understanding the gating of both hyperpolarizing and depolarizing MSCs. Besides prototypical activation by membrane tension, additional gating mechanisms involving channel curvature and/or tethered elements are at play.

Opening of MSCs at the plasma membrane of mammalian cells, in the microseconds range, is the earliest event occurring upon mechanical stimulation (Chalfie, 2009; Christensen and Corey, 2007; Delmas and Coste, 2013; Kung, 2005; Murthy et al., 2017; Sachs and Morris, 1998). Activation of MSCs by force is direct without the involvement of a second messenger, causing a change in membrane potential and triggering biochemical responses (Kung, 2005; Sachs and Morris, 1998). In mammalian cells two types of MSCs co-exist at the plasma membrane: the depolarizing cationic non-selective channels (permeable to Na^+, K^+ and Ca^{2+}) and the hyperpolarizing K^+-selective stretch-activated channels (Delmas and Coste, 2013; Murthy et al., 2017)(Figure 1; Key table). MSCs open in response to a variety of mechanical stimuli, including local membrane stretching, cell squeezing, shear stress, cell swelling, deflection of hair cell bundles, as well as substrate deformation (Delmas and Coste, 2013; Wu et al., 2017a).

In this review, taking advantage of recent molecular, structural and functional studies, we will discuss the common properties, as well as the specific gating mechanisms that are involved in the activation of the different types of mammalian MSCs by force, including TREK/TRAAK K_{2P} channels, Piezo1/2, TMEM63/OSCA and TMC1/2 (Figure 1, Key table), in light of their physiological role and association with various disease states.

Activation of MSCs by membrane tension

The prototypical bacterial MscL channel, acting as an osmotic valve, is a very large conductance (3 nS) ionic pore permeable to both ions (without selectivity) and osmolytes that is gated by membrane tension (Kung, 2005; Sukharev et al., 1994)(Figure 2B). Activation involves a major iris-like expansion of its transmembrane segments (TMs) (Perozo et al., 2002). Force is directly transmitted to the channel through the membrane ("force-from-lipid principle")(Kung, 2005; Martinac et al., 1990). A large increase in channel cross-sectional area (about 20 nm^2 for MscL), caused by an increase in membrane tension, confers a high mechanosensitivity; proportional to the steepness of the sigmoidal gating curve primarily reflecting the dimensional changes of the mechanosensitive channel upon force activation (Sukharev et al., 1994)(Figure 2A). In comparison, for small conductance (about 100 pS; 30 fold less than MscL) mammalian TREK-1/TREK-2/TRAAK $K2_P$ channels, only a modest increase in cross-sectional area (1.8, 2.7 and 4.7 nm^2 for TREK-1, TRAAK and TREK-2, respectively) is occurring (Brohawn et al., 2014a; Dong et al., 2015; Honoré et al., 2006)(Figure 2B). Thus, large conductance MSCs are sensitive to smaller changes in membrane tension than small conductance MSCs. If the MSC in the bilayer is approximated to a cylindrical plug, the free energy difference between the open and closed states ($\Delta G = \Delta G0 - T\Delta A$) is given by $\Delta G0$ [the difference in the absence of force] minus membrane tension (T) times the change in cross-sectional channel area occurring between the closed and the open state [ΔA] (Liang and Howard, 2018; Sachs and Morris, 1998). Tension causes an expansion (ΔA) of the mechanosensitive channel (inducing pore opening) by an energy equal to $-T\Delta A$. Protein area expansion (ΔA) is proportional to the energy that controls activation of the channel. Thus, a smaller area change (ΔA) requires a broader range of tension (between 0.5 and 12 mN/m for TRAAK) for channel activation (shallow gating curve) (Brohawn et al., 2014a; Dong et al., 2015; Honoré et al., 2006)(Figure 2A). Notably, both positive and negative pressure (causing a similar increase in membrane tension) activates reconstituted TRAAK channels (Brohawn et al., 2014b).

In summary, two MSC classes that appear to have different degrees of cross-sectional area changes, bacterial MscL and mammalian mechanosensitive TREK/TRAAK K_{2P} channels, offer good examples of how variations in this key parameter that controls "force-from-lipid" manifest (Figure 2A).

Threshold for mechanical activation of MSCs

Besides the steepness of the gating curve (related to the difference in cross-sectional area changes), another striking difference between MscL and mechanosensitive K_{2P} channels is the threshold for mechanical activation that is very high for MscL (10 mN/m), but remarkably low for TRAAK (0.5 mN/m)(Aryal et al., 2017; Brohawn et al., 2014a; Brohawn et al., 2014b; Sukharev et al., 1994)(Figure

2A). The mid-point of the gating curve depends on channel pre-stress (i.e. the resting tension acting on the channel), influenced by the stiffness of the membrane and the cytoskeleton linkages (Sachs and Morris, 1998). For mechanosensitive TREK/TRAAK K_{2P} channels, modest channel area expansion together with a reduced lipid deformation are proposed to synergistically promote channel activation in the lower tension range (Brohawn et al., 2014a). Thus, both protein expansion (ΔA) and pre-stress are key parameters conditioning the gating of MSCs.

HYPERPOLARIZING MECHANOSENSITIVE MAMMALIAN K_{2P} POTASSIUM CHANNELS

K_{2P} channels in physiology and disease states

Opening of TREK/TRAAK K_{2P} channels results in an efflux of potassium causing cell hyperpolarization and a consequent decrease in cell excitability (for review see (Honoré, 2007)). TREK/TRAAK are polymodal K^+ channels that are stimulated by protons, heat, stretch, and a variety of lipids including free polyunsaturated fatty acids (PUFAs), lysopholipids, PIP_2, lysophosphatidic acid and phosphatidic acid, as well as pharmacological agents such as volatile general anaesthetics (for review, (Honoré, 2007)). On the contrary, TREK-1 is negatively regulated through phosphorylation by protein kinases A and C (for review, (Honoré, 2007)). Both TREK-1/2 and TRAAK are highly expressed in neurons, including sensory dorsal root ganglion neurons (Key Table). TREK-1/TRAAK knock-out mice show enhanced sensitivity to painful stimuli, including mechanical allodynia, as well as heat-hyperalgesia (Alloui et al., 2006; Noel et al., 2009). Moreover, TREK-1 knock-out mice are sensitized to inflammatory pain (Alloui et al., 2006; Noel et al., 2009). In the same line, TREK-1 plays a role in migraine (Royal et al., 2019). Opening of hyperpolarizing K_{2P} channels limits (acting as an electrical brake) the depolarization mediated by the activation of other types of excitatory cationic non-selective channels, including MSCs and heat-sensitive TPRV channels. Thus, TREK/TRAAK MSCs are involved in polymodal pain perception (Alloui et al., 2006; Noel et al., 2009). Of note, within the central nervous system, TREK-1 is also involved in neuroprotection, general anaesthesia and plays an important role in depression (for review see (Honoré, 2007)).

Interestingly, missense mutations (Ala172Glu and Ala244Pro, in TM3 and TM4, respectively) in TRAAK cause a syndrome including facial dysmorphism hypertrichosis, epilepsy, intellectual disability/developmental delay, and gingival overgrowth (Bauer et al., 2018)(Key Table). Those mutations produce a basal gain-of-function (GOF) that impairs sensitivity to mechanical stimulation, as well as activation by arachidonic acid. MD simulations predict that the TRAAK disease-causing mutations seal lateral fenestrations (Aryal et al., 2017; Bauer et al., 2018; Brohawn et al., 2014a)(Figure 1A and see below).

Thus, hyperpolarizing mechanosensitive K_{2P} channels play a major pathophysiological role and are implicated in a variety of inherited and acquired disease states.

Gating of mechanosensitive K_{2P} channels involves a large conformational change in TM4

The K_{2P} channels TREK-1/TREK-2/TRAAK are made of a dimer of subunits, each including four transmembrane segments (TMs) and two pore domains (P1-P2) in tandem (Brohawn et al., 2014a; Brohawn et al., 2012)(Figure 1A). A large extracellular cap with a bifurcated ionic pathway lies on top of the transmembrane channel core, thus explaining their resistance to K^+ channel pore blockers (Brohawn et al., 2012)(Figures 1A and 3). Notably, K_{2P} channels lack a classical bundle-crossing inner gate, as found in other types of K^+ channels. An upward movement of the inner end of TM4 due to a rotation (25°) around a central hinge glycine, together with a rotation (15°) of the TM2-TM 3 segments, obstruct two large intramembrane-side fenestrations (Brohawn et al., 2014a)(Figure 1A, Figure 3A). When TM4 is in the down state (dashed magenta line), lateral windows are wide open (yellow circle) and it was hypothesized that they might be filled with lipids (in yellow) extending to the central cavity underneath the selectivity filter, presumably blocking the flow of K^+ ions (Brohawn et al., 2014a)(Figure 1A, middle, Figure 3A). In response to an increase in membrane tension, it is predicted that lateral fenestrations close because of an upward movement of TM4 (no dash magenta line), thereby preventing the entry of blocking lipids and allowing the flow of K^+ (Brohawn et al., 2014a)(Figure 1A, right panel, Figure 3A). However, molecular dynamics (MD) simulations of TREK-2 predict that phospholipid tails appear to be too short to reach into the cavity (Aryal et al., 2017). Moreover, intracellular Rb^+ activates TREK-1 by directly influencing a voltage-dependent gate within the selectivity filter, even in the absence of stretch (i.e. when TM4 is in the down state and when lateral fenestrations are opened) (Aryal et al., 2017; Schewe et al., 2016). Thus, these electrophysiological data are not consistent with a lipid occlusion model since intracellular Rb^+ would be unable to reach the selectivity filter if lipids block the permeation pathway (Aryal et al., 2017). While a large conformational change in TM4 (controlling the opening of lateral fenestrations) occurs upon channel activation, more recent findings strongly support the notion that the activation gate is located at the level of the selectivity filter (Lolicato et al., 2017)(Figure 3B).

Gating of TREK/TRAAK channels by a selectivity filter C-type gate

Norfluoxetine (Prozac) only binds and inhibits TREK-2 when the lateral fenestrations are opened (i.e. when TM4 is down) (Dong et al., 2015; McClenaghan et al., 2016)(Figure 3). Taking advantage of the state dependent inhibition of TREK-2 by norfluoxetine, it was demonstrated that TREK-2 can be conductive both when TM4 is down or up (Lolicato et al., 2014; McClenaghan et al., 2016)(Figure 3B). Additional findings indicate that the selectivity filter of mechanosensitive K_{2P} channels acts as an

activation gate (C-type gate) (Bagriantsev et al., 2012; Bagriantsev et al., 2011; Lolicato et al., 2017; McClenaghan et al., 2016)(Figure 3B). Notably, binding of small molecule TREK-1 activators (ML335 and ML402) to a cryptic binding pocket (between P1 pore helix and TM4) is predicted to restrict the movement behind the selectivity filter, enhancing K^+ permeation (Lolicato et al., 2017)(Figure 3B). Moreover, MD simulations predict that membrane stretch increases K^+ occupancy within the selectivity filter of TREK-2 (Aryal et al., 2017).

Notably, mechanosensitive K_{2P} currents show a relaxation during maintained pressure stimulation, both in transfected cells or upon reconstitution into artificial bilayers (Brohawn et al., 2014b; Honoré et al., 2006). This inactivation mechanism (τ: 45 ms) is intrinsic to the channel, and is sensitive to pre-stress (resting tension) and resembles the C-type inactivation of Kv channels, a process by which K^+ flux is blocked by conformational changes of the selectivity filter (Brohawn et al., 2014b; Honoré et al., 2006).

Altogether, those findings indicate the contribution of a filter C-type gate, as well as of a large conformational change of the TM4 helix, in the gating of mechanosensitive K_{2P} channels (Brohawn et al., 2014a; Lolicato et al., 2017; Lolicato et al., 2014; McClenaghan et al., 2016)(Figure 1A and Figures 3A-B). In addition, the TREK-1 intracellular C-terminal cytosolic domain is a major regulatory element of the channel and relays mechanical, thermal and acidic modulations to the filter C-type gate through transmembrane helix TM4 and pore helix 1 (Bagriantsev et al., 2012; Bagriantsev et al., 2011)(Figure 3C, dashed arrows). Conversely, phosphorylation of the Ct domain at Ser 300 and Ser 333 by protein kinases A or C inhibits channel activity (for review (Honoré, 2007))(Figure 3C).

TREK activation by asymmetry of the transbilayer pressure profile

Across the lipid bilayer there is repulsion between the head groups and between the lipid tails generating positive pressure (push), while there are two regions of high negative pressure (pull) around the glycerol backbone that is required to prevent water entry through the membrane (Aryal et al., 2017; Clausen et al., 2017; Martinac et al., 2018)(Figure 2D). Upon stretch of an ideal membrane, thickness is reduced, the positive pressure in the middle of the bilayer is lowered, while the peaks of negative pressure are increased (Aryal et al., 2017)(Figure 2D). In MD simulations of TREK-2, a change in the lateral pressure profile (by lowering the number of phospholipids in the inner leaflet, but not in the outer leaflet) is sufficient to induce an upward movement of TM4, while reducing bilayer thickness (i.e. hydrophobic mismatch) was not sufficient to drive this structural transition (Aryal et al., 2017). Moreover, reconstituted TREK-2 channels in a planar bilayer differentially respond to positive and negative pressure, suggesting a sensitivity to transbilayer pressure profile asymmetry (Clausen et al., 2017). These findings fit with the activation of TREK-1 by external, rather than internal lysophosphatidylcholine (LPC), as well as with the stimulation by

anionic amphipaths (including arachidonic acid), but inhibition by cationic amphipaths (including chlorpromazine) (Maingret et al., 2000). Increased free volume within the inner leaflet is anticipated to promote expansion of the lower end of the TREK/TRAAK channels (ΔA), mainly due to the upward movement of TM4 (Aryal et al., 2017; Brohawn et al., 2014a)(Figure 2C and Figure 3A).

Thus, TREK/TRAAK channels show an asymmetric mechanosensitivity, as previously reported for the bacterial MscL channel (Martinac et al., 2018)(Figures 2C-D). However, some MSCs are more sensitive to stress in the inner compared to outer monolayer, whereas the sensitivity of others is the opposite.

DEPOLARIZING NON-SELECTIVE CATIONIC PIEZO CHANNELS

Role of Piezo1/2 in mechanosensory physiology and disease states

Opening of Piezo1/2 channels is involved in a variety of key physiological functions and disease states (recently extensively reviewed elsewhere (Murthy et al., 2017)). In particular, Piezo1 plays a major role in vascular development and physiopathlogy. In brief, Piezo1 expression in the endothelium is required for early vasculogenesis (constitutive knock-out is embryonic lethal) and is involved in flow-dependent vasodilatation at the adult stage (Li et al., 2014; Ranade et al., 2014a; Wang et al., 2016)(Key Figure). By contrast, endothelial Piezo1 mediates vasoconstriction of mesenteric arteries during whole body physical activity associated with high blood flow through, in this case, depolarization of vascular smooth muscle cells electrically connected to the endothelium via gap junctions (Rode et al., 2017). In addition, Piezo1 opening in smooth muscle cells profoundly affects the structural remodeling of small diameter arteries upon hypertension (Retailleau et al., 2015). Piezo1 is also involved in the formation of both lymphatic and aortic valves (Nonomura et al., 2018) (https://doi.org/10.1101/528588; https://doi.org/10.1101/529016). Finally, opening of Piezo1 causes red blood cell (RBC) dehydration by an efflux of potassium through calcium dependent activation of the Gardos K^+ channel (KCNN4), while Piezo1 deletion in RBCs leads to overhydration (Cahalan et al., 2015)(Key table).

Piezo2 is highly expressed in two skin cell types: both low threshold mechanoreceptors (large diameter DRG neurons) that innervate the skin and in Merkel cells (tactile epithelial cells). Piezo2 is responsible for light touch sensation, although it is not critically required for mechanical nociception (Maksimovic et al., 2014; Murthy et al., 2018b; Ranade et al., 2014b; Szczot et al., 2018; Woo et al., 2014)(Key table). However, Piezo2 is involved in mechanical allodynia (increased response of neurons to mechanical stimulation) under skin inflammatory conditions or nerve injury (Murthy et al., 2018b; Szczot et al., 2018). Piezo2 is also expressed in muscle spindles, the sensory nerve endings innervating skeletal muscles that are responsible for proprioception and required for proper control

of limb position and coordination (Woo et al., 2015). In addition, Piezo2 is found in vagal sensory neurons innervating the airway where it mediates the autonomic reflex of lung inflation-induced apnoea (Nonomura et al., 2017). Finally, both Piezo1 and Piezo2 are acting in parallel in the baroreceptors of the aorta and carotid sinus, with a critical role for the acute control of blood pressure (Zeng et al., 2018). Notably, mice that lack Piezo1/2 show labile hypertension and increased blood pressure variability (Zeng et al., 2018)(Key table).

Various inherited diseases are associated with mutations in Piezo1/2 genes (Key table). Slower Piezo1 inactivation caused by GOF dominant mutations leads to xerocytosis, an hemolytic anemia associated with dehydration of RBCs (Albuisson et al., 2013; Bae et al., 2013; Zarychanski et al., 2012). Interestingly, one such common GOF Piezo1 allele in African populations confers a significant protection against *Plasmodium falciparum* infection (Ma et al., 2018). Recessive loss-of-function mutations (LOF) in Piezo1 are associated with lymphatic dysplasia (lymphedema) (Lukacs et al., 2015). Concerning Piezo2, dominant GOF mutations cause distal arthrogryposis (contractures that restrict movement in the hands and feet)(Coste et al., 2013), while recessive LOF mutations are associated with a syndrome of muscular atrophy with perinatal respiratory distress, arthrogryposis and scoliosis (Delle Vedove et al., 2016; Haliloglu et al., 2017).

In addition, Piezo1/2 are also anticipated to play an important role in several acquired diseases, including cancer and pancreatitis (Chen et al., 2018; Romac et al., 2018).

Those findings indicate that Piezo1/2 are associated with a variety of clinical disorders, as anticipated with their specific patterns of expression (Key table).

The low threshold cationic non-selective Piezo1 channel is inherently mechanosensitive

Piezo1/2 channels (47% identity) are low threshold (1-3 mN/m), fast inactivating (τ of about 25 ms), small conductance (about 35 pS) depolarizing mechanically activated non-selective cationic channels permeable to sodium, potassium and calcium (Coste et al., 2010; Cox et al., 2016; Lewis and Grandl, 2015; Syeda et al., 2016)(Key table). Piezo channels are conserved during evolution and found in plants, ciliated protozoans, *Drosophila*, as well as *C.elegans*. Piezo1 is inherently mechanosensitive, as demonstrated by reconstitution experiments into artificial bilayers (Syeda et al., 2016). In a symmetrical phosphatidylcholine (PC/PC) bilayer Piezo1 is closed, while it shows basal openings (i.e. activity without mechanical stimulation) when the cis leaflet is doped with lysophosphatidic acid (LPA) (Syeda et al., 2016). Moreover, Piezo1 opening was enhanced in a symmetrical PC/PC bilayer by osmotic stress and by solvent injection-mediated monolayer expansion. Piezo1 is activated by both negative or positive pressure applied in the cell-attached patch clamp configuration (Coste et al., 2010). By contrast, Piezo2 opens in response to positive, but not negative, pressure (Shin et al., 2019).

These observations indicate that Piezo1 is intrinsically mechanosensitive and directly activated by membrane tension (Cox et al., 2016; Lewis and Grandl, 2015; Syeda et al., 2016).

Sensing force by a change in Piezo1 curvature

The 3D structure of mPiezo1 was solved by cryo-electron microscopy, revealing a very large trimeric ion channel complex (about 900 kDa), with an unusual curved shape (Ge et al., 2015; Guo and MacKinnon, 2017; Saotome et al., 2018; Zhao et al., 2018)(Figures 1B and 4). The complex is a trimer of Piezo1 subunits with three large distal flexible blades (each containing 9 repeats of 4 TMs) and an extracellular carboxy terminal domain (CED) at the centre of the complex connected by flexible linkers to the last two TMs (outer and inner helices) (Ge et al., 2015)(Figure 1B). The C terminal end of the protein constitutes a central pore module, whereas the remaining N terminal non-pore region is proposed to act as an independent mechanosensitive module (Zhao et al., 2016). Very recently the near-complete structure of Piezo2 was solved, similar to Piezo1, comprising 114 transmembrane helices in total (Wang et al., 2019). A chimera between the N terminal domain of Piezo1 with ASIC1 was claimed to be mechanosensitive (Zhao et al., 2016), although this finding could not be confirmed by others (Dubin et al., 2017). Nevertheless, the central pore domain and the role of the amino terminal domain in mechanosensing were further demonstrated by elegant structural studies and mutational analysis (Guo and MacKinnon, 2017; Saotome et al., 2018; Zhao et al., 2018). The ionic pore is made of the three inner helices (IH) with hydrophobic residues facing the cavity. The wall of the pore is not completely sealed and isolated from the membrane, suggesting that membrane lipids might influence permeation (as proposed for TRAAK)(Saotome et al., 2018)(Figure 1B, right panel). Cations might flow laterally between the CED and the transmembrane portion of the channel (Figure 4A). Piezo1 is constricted at the lower end of the pore by the residues Met 2493, Pro 2536 and Glu 2537 (Guo and MacKinnon, 2017; Saotome et al., 2018) (Figures 1B and 4A). In comparison, the transmembrane part of Piezo2 is completely sealed (Wang et al., 2019). Moreover, besides the inner constriction site, as found in Piezo1 (Fig. 1B), an upper constriction formed by Leu 2743 is also present in Piezo2 (Wang et al., 2019). In the open state, the diameter of the Piezo1 pore is expected to increase at least to a radius of 4 Å, based on ionic selectivity. A long inner helix of 66 amino acids, called the beam, extends from the center and is parallel to the membrane (Zhao et al., 2018)(Figures 1B and 4A). Viewed from the side, the Piezo1 timer is curved into a dome shape with a 60° angle between the beam and the central axis of the pore (Guo and MacKinnon, 2017; Haselwandter and MacKinnon, 2018; Liang and Howard, 2018)(Figures 4A-B). Remarkably, mPiezo1 trimers deform the lipid bilayer locally into a dome when reconstituted into unilamellar vesicles (Guo and MacKinnon, 2017)(Figure 4B). Furthermore, mechanical calculations predict that Piezo1 will shape the membrane into a curved “membrane footprint”, thus influencing the mechanics of the bilayer at a distance from

the channel and amplifying the mechanosensitivity of Piezo1 in the low tensional range (Haselwandter and MacKinnon, 2018). It is hypothesized that Piezo1 may sense membrane tension though a flattening, with a consequent large increase in the in-plane channel area (ΔA) (Haselwandter and MacKinnon, 2018; Liang and Howard, 2018)(Figure 4D). If Piezo1 becomes completely flat in response to an increase in tension, its cross-sectional area (ΔA) is expected to increase by 120 nm^2 (versus 20 nm^2 for MscL and 4.8 nm^2 for TRAAK). This estimated large increase in ΔA is predicted to confer exquisite mechanosensitivity to Piezo1 (i.e. the driving energy $-T\Delta A$ is high), despite the fact that Piezo1 has a small ionic pore (35 pS) (Liang and Howard, 2018). Extracellular loops TMs 15-16 and 19-20 are critically required for mechanical activation of Piezo1 (as well as for activation by Jedi1 and Jedi2), although mutants in this region remain normally activated by the small molecule activator Yoda1 (Syeda et al., 2015; Zhao et al., 2018)(Figure 4A; in magenta). The intracellular beam is anticipated to act as a long distance transduction element between the peripheral mechanosensitive blades (TMs 15-16 and 19-20) to the central pore module, behaving as a lever around a proximal pivot (Leu 1342 and Leu 1345) that controls pore opening (Zhao et al., 2018)(Figure 4A, in red). Leu 2475 and Val 2476 in the intracellular C-terminal domain (CTD) form a primary hydrophobic inactivation gate and Met 2493/Phe 2494 hydrophobic constriction acts as a secondary inactivation gate in Piezo1 (Zheng et al., 2019).

Altogether, these findings indicate that Piezo1 might sense membrane tension through a change in its curvature (Guo and MacKinnon, 2017; Liang and Howard, 2018)(Figures 4B-D). Indeed, recent cryo-electron microscopy observations, as well as atomic force microscopy analysis demonstrate that Piezo1 can be flattened reversibly into the membrane plane (Lin et al., 2019).

Regulation of Piezo1/2 mechanosensitivity by lipids

A lipid shaped density was observed in an apparent ligand-binding pocket between the anchor and the first repeat of the blade with two arginines (R2035 and R2135) projecting into the pocket (Saotome et al., 2018)(Figure 4A; in gray). Mutations of Arg 2135 killed channel activity, suggesting that interaction with lipids might play an important regulatory role in the regulation of Piezo1 (Saotome et al., 2018). In line with these findings, incorporation of saturated margaric acid (MA; C17:0) into phospholipids inhibits Piezo1 activation, while long chain polyunsaturated fatty acid docosahexaenoic acid (DHA; C22:6) slows the inactivation rate of Piezo1 (Romero et al., 2019). Thus, depending on the chain length and unsaturation, fatty acids differentially regulate Piezo1 gating. Decreased Piezo1 opening when phospholipipds are enriched in MA correlates with an increase in membrane rigidity, possibly restricting Piezo1 in-plane area expansion, despite an anticipated increase in pre-stress (see above) (Romero et al., 2019). DHA might slow down Piezo1 inactivation by

reducing the cohesion between phospholipids and the transmembrane domain to stabilize the open state of the channel (Romero et al., 2019).

In the same line, depletion of cholesterol and deficiency of STOML3 similarly and interdependently attenuate the mechanosensitivity of Piezo1 (Poole et al., 2014; Qi et al., 2015; Wetzel et al., 2017). In addition, super resolution imaging also demonstrates that cholesterol depletion increases Piezo1 diffusion in live cells (https://doi.org/10.1101/604488).

TMEM150C, initially claimed to be an independent slow-adapting mechanosensitive ion channel in DRG neurons, instead acts as a general regulator of other force-gated ion channels, slowing down the inactivation rates of both Piezo1/2 and TREK-1 (Anderson et al., 2018; Hong et al., 2016). Since the TMEM150A homologue modulates phospholipid homeostasis, it is suggested that TMEM150C might similarly influence membrane lipid composition and possibly modulate the gating of MSCs (Anderson et al., 2018).

Thus, Piezo1 mechanosensitivity and kinetics are greatly influenced by the membrane lipid composition.

In summary, Piezo1/2 channels are low threshold non-selective cationic depolarizing channels (Key table). Piezo1 has a trimeric structure that curves the membrane in the closed state. An open state structure of Piezo1 is required to confirm the hypothesis of tension-dependent channel flattening (Guo and MacKinnon, 2017; Liang and Howard, 2018). If Piezo1 is able to dynamically alter membrane curvature, it is anticipated that neighboring proteins (including other Piezo1 molecules, other types of MSCs, or curvature sensitive molecules) within the membrane footprint will also be influenced and might act in concert with Piezo1 in response to mechanical stimulation (Haselwandter and MacKinnon, 2018).

Several recent studies identified a new class of high threshold non-selective cationic channels, present in plants (OSCA), as well as in mammals (TMEM63), that might act in parallel with Piezo1.

THE HIGH THRESHOLD NON-SELECTIVE CATIONIC MSCs TMEM63/OSCA

The hyperosmolarity-evoked intracellular calcium response in plants is mediated by AtOSCA1 (Yuan et al., 2014). Recent reports indicate that both AtOSCA1.1 and AtOSCA1.2 from *Arabidopsis thaliana* are pore-forming subunits in transfected HEK cells that are activated by mechanical stimulation (Jojoa-Cruz et al., 2018; Liu et al., 2018; Murthy et al., 2018a; Zhang et al., 2018)(Figure 1C). AtOSCAs evoke high-threshold mechano-activated currents ($P_{0.5}$ of about -55 mm Hg) with kinetics of inactivation comparable to Piezo1 (τ of about 25 ms)(Murthy et al., 2018a; Zhang et al., 2018). Of note, the single channel conductance of OSCA channels is too small to be resolved. OSCAs are

cationic non-selective with a slight permeability for chloride. Reconstitution of purified AtOSCA1.2 into artificial bilayers induces robust stretch activated currents, demonstrating that this protein is intrinsically mechanosensitive (Murthy et al., 2018a). Moreover, as previously reported for other MSCs, LPC addition increased the mechanosensitivity of OSCA channels, indicating that this channel might also be sensitive to the local bilayer curvature/asymmetry of the transbilayer pressure profile (Martinac et al., 2018; Zhang et al., 2018).

Notably, the human and mouse homologues TMEM63a,b,c give rise to slowly or non-inactivating high threshold cationic non-selective mechanosensitive currents (Murthy et al., 2018a)(Key table).

Structure of the OSCA MSCs

AtOSCA1.1, AtOSCA3.1 and AtOSCA1.2 are dimers with a two-fold symmetry axis perpendicular to the membrane, with each subunit comprising 11 TMs and a pore domain (Jojoa-Cruz et al., 2018; Liu et al., 2018; Maity et al., 2019; Zhang et al., 2018)(Figure 1C). Both subunits are separated by a large central cavity filled with lipids that might help stabilize the complex. The cytosolic domain is made of the TM2-TM3 loop and the C terminus (Jojoa-Cruz et al., 2018; Liu et al., 2018; Zhang et al., 2018)(Figures 5A-B). OSCAs have structural similarities to the calcium-activated chloride channels TMEM16 family of proteins, with a dual pore, despite an additional TM segment (TM0), the absence of regulatory negatively charged calcium binding site and structural differences in the cytosolic domain. TM3-TM7 forms the pore and a hydrophobic ring creates a constriction at the extracellular end of the pore (Jojoa-Cruz et al., 2018; Liu et al., 2018; Zhang et al., 2018)(Figure 1C, right panel). Since OSCA1.1 conducts gluconate, its open pore diameter is at least 5.5 Å, indicating that the solved structures are all in the closed state. MD simulations predict that the hydrophobic neck is predicted to widen when membrane tension increases (Zhang et al., 2018). Below the hydrophobic neck, Glu 462 at the base of TM5 in OSCA1.1 and Glu 531 on TM6 in OSCA1.2 protrude in the hydrophilic pore cavity and greatly influence single channel conductance, demonstrating that this region indeed directly contributes to the ionic pore (Jojoa-Cruz et al., 2018; Zhang et al., 2018). A putative activation model of OSCAs involves both straightening of TM6 and bending of TM0, causing an opening of the activation gate (Zhang et al., 2018). Interestingly, the lower region of the pore is also directly exposed to lipids through a large fenestration, due to the separation between TM5 and TM7 (Jojoa-Cruz et al., 2018)(Figure 1C, right panel). A distinctive feature in OSCAs (but absent in OSCA2.2) is the presence of a large hook shape cytosolic loop (within TM2-TM3) that contains a hydrophobic sequence, presumably buried in lipids (Jojoa-Cruz et al., 2018)(Figure 5B). Local change of this membrane anchor in response to increased tension might contribute to channel activation (Liu et al., 2018).

Thus, TMEM63/OSCAs constitute a novel structural class of MSCs, including two pores per channel (Figures 1C and 5B). At this stage the physiological relevance of the high threshold slowly inactivating mammalian TMEM63a,b,c isoforms is unknown and needs to be explored in future studies.

THE MET CHANNEL OF HAIR CELLS: A TETHERED MSC

Inner ear hair cells are the specialized mechanosensory cells responsible for hearing and balance, within the cochlea and the vestibular system, respectively (Fettiplace, 2016; Gillespie and Muller, 2009; Hudspeth et al., 2000). Hair cells are equipped at their apical side with several rows of stereocilia forming a hair bundle, arranged in a staircase of decreasing heights (Gillespie and Muller, 2009)(Figure 5D). The mechanoelectrical transduction (MET) channel is located at the tips of all but the tallest stereocilia. Deflection of the bundle towards the tallest stereocilia opens the MET channels, while deflection towards the shortest allows them to close (Corey and Hudspeth, 1979)(Figure 5D). The tip link (low compliance), between two neighboring stereocilia, pulls on the MET channel (Figure 5D). Accordingly the MET current is lost when the tip link is disrupted by chelating calcium with BAPTA. The tip link is made of a homodimer of cadherin 23 (CDH23) at the upper end anchored to the stereocilium through the Usher complex Myo7a along with other myosins, and protocadherin related 15 (PCDH15) at the lower end interacting with the MET channel (Fettiplace, 2016; Ge et al., 2018; Maeda et al., 2014; Qiu and Muller, 2018; Richardson et al., 2011)(Figure 5D). The MET channel opens in the microseconds range following positive deflection of the hair cell bundle, indicating that channel mechanical activation is direct (i.e. without the involvement of a second messenger)(Christensen and Corey, 2007). The hair cell transduction channel has a large conductance (about 200 pS), is cationic non-selective with a high permeability to calcium, and also is permeable to some large fluorescent molecules, including FM1-43 (Fettiplace, 2016; Qiu and Muller, 2018). *In vivo*, the hair cell MET channel mainly conducts potassium because this is the most abundant cation of the fluid bathing stereocilia (endolymph). High frequency sounds are detected at the base, while low frequency tones at the apex of the organ of Corti (for reviews: (Fettiplace, 2016; Gillespie and Muller, 2009; Qiu and Muller, 2018)). This is paralleled by a tonotopic gradient of single channel conductance in outer hair cells (unlike inner hair cells), with larger single MET channel conductance at the base (about 160 pS) of the cochlea, as compared to the apex (about 70 pS) (Beurg et al., 2018; Pan et al., 2013). A key characteristic of the MET channel is a complex adaptation mechanism in response to hair bundle deflection that causes a gradual decrease in current amplitude, involving both a fast adaptation (about 1 ms; possibly involving calcium, PIP_2 or other factors) and a slower mechanism (about 20 ms; likely regulated by myosin motors at the upper insertion site of the tip link) (Fettiplace, 2016; Gillespie and Muller, 2009; Qiu and Muller, 2018).

TMC1 is a key component of the MET channel ionic pore

Molecular identification of the MET channel in hair cells has been a major challenge over the years due to the small amount of tissue available, low number of channels per hair cell, molecular complexity and difficulty of expressing channel subunits using classical heterologous systems (Corey and Hudspeth, 1979; Fettiplace, 2016; Gillespie and Muller, 2009).

Several lines of evidence now support a key role for transmembrane channel-like proteins 1 and 2 (TMC1 and TMC2) as the pore-forming proteins of the MET channel complex (Kawashima et al., 2011; Pan et al., 2018; Pan et al., 2013)(Figure 5C-D; Key table). TMC2 is expressed transiently after birth in mammalian cochlear hair cells, while TMC1 is expressed later in hair cells and maintained throughout the adult stage (Li et al., 2019). TMC1/2 localize at the tip of the lower stereocilia of both outer and inner hair cells and biochemical interaction was shown between the C terminal region of PCDH15 (a component of the tip link) and the first N terminal 179 and 232 amino acids (presumably intracellular) in mTMC1 and mTMC2, respectively (Li et al., 2019; Maeda et al., 2014)(Figure 5C-D). Notably, the *Beethoven* deafness-causing dominant mutation in TMC1 alters calcium permeability of the MET channel (for review, (Fettiplace, 2016))(Figure 5E). Moreover, the MET current is fully suppressed in the double *Tmc1*/*Tmc2* knock-out mice, causing severe hearing and balance deficits, but can be rescued by adeno-associated viral (AAV) vectors expressing TMC1 or TMC2 (Kawashima et al., 2011; Nist-Lund et al., 2019; Pan et al., 2018; Pan et al., 2013). Altogether these observations strongly suggest that TMC1/2 is a key component of the MET channel (Pan et al., 2018). Of note, the gradient of single channel conductance in outer hair cells along the chochlea (tonotopic gradient) was attributed to the TMC1/TMC2 stoichiometry or to a variable number of TMC1 channels (Beurg et al., 2018; Pan et al., 2013).

Recent evidence indicates that TMC1 assembles as a dimer with structural similarity to TMEM16 and TMEM63/OSCA (Ballesteros et al., 2018; Pan et al., 2018)(Figure 1D and Figures 5A and C). Recently, cysteine mutagenesis was elegantly used to map the pore of TMC1, taking advantage of a complementation assay in double *Tmc1*/*Tmc2* knock-out mice with AAV delivery of mutant *Tmc1* constructs (Pan et al., 2018)(Figure 5E). This laborious assay was needed because TMCs do not reach the plasma membrane when transfected into anything other than hair cells. MET currents were recorded before and after addition of cysteine reagents. Addition of 2-(trimethylammonium)-ethyl methanethiosulfonate (MTSET), that forms covalent linkage with cysteines, reduced transduction current in several mutants, suggesting their likely contribution to the ionic pore (Pan et al., 2018)(Figure 5E). Importantly, cysteine modification also decreased calcium selectivity of the transduction channel in eight of the mutants within TM4-7 (including, Asn404Cyst, Gly411Cyst, Thr531Cyst and Thr532Cyst)(Figure 5E). All identified residues that altered permeation properties are

predicted to face a large pore anionic cavity, while nonreactive residues face away or are distant from the pore (Pan et al., 2018). Notably, open-channel blockers, as well as channel closure by negative deflection of the hair cell bundle, prevented access of MTSET to cysteine residues lining the pore (Pan et al., 2018). In particular, the *Beethoven* mutation (Met418Lys in hTMC1 and Met412Lys in mTMC1) similarly lines the predicted pore in the modeled TMC1 channel (Pan et al., 2018)(Figure 5E). These key findings indicate that TMC1 is a pore-forming component of the MET channel, although it does not exclude that other transmembrane proteins (including TMHS, TMIE and/or PCDH15) might also be involved (Pan et al., 2018; Qiu and Muller, 2018). TMHS (LHFPL5) that is co-localized with TMC1 at the tip of the lower stereocilia might functionally couple the tip link to the transduction channel (i.e. to TMC1) and/or acquiring/maintaining TMC1 localization, although PCDH15 also binds TMC1 directly (Ge et al., 2018; Maeda et al., 2014)(Figures 5C-D). Since PCDH15 has a cis-dimeric architecture, there is a possibility that each helix might connect with a TMC1/2 monomer within the MET channel complex (Dionne et al., 2018; Pan et al., 2018). Altogether these recent findings indicate that TMC1/2 are pore-forming components of the MET channel, with a structure comparable to TMEM63/OSCA (Figures 1C-D; Figures 5A and C).

Of note, Piezo2 is also present at the apical side of the hair cell, but at the base of the stereocilia and its opening is caused by negative pressure near the apical surface, as well as by displacement of the bundle towards the shortest stereocilia (reverse polarity), independently of the tip link (Wu et al., 2017b). Auditory function is only mildly altered by knock-out of Piezo2 and a role in the continuous repair of the sensory transduction apparatus was instead suggested (Wu et al., 2017b).

Conclusions and perspectives

Among the different classes of mammalian MSCs, the highest similarity is predicted between TMEM63/OSCA and TMC1/2, despite the fact that force transmitted to the channel originates from the bilayer in the case of OSCAs, but from a tip link (tether) for TMCs (Ballesteros et al., 2018; Jojoa-Cruz et al., 2018; Liu et al., 2018; Pan et al., 2018; Zhang et al., 2018). Whether or not the tip link directly gates the channel and/or generates a local change in membrane tension (PCDH15 has a C terminal transmembrane domain (Qiu and Muller, 2018)) that in turn activates TMC1 is unclear at this stage. Since TMC1 shows structural similarity with OSCA channels (Figures 1C-D), the force-from-lipid model should not be overlooked in the context of the hair cell MET channel (Jojoa-Cruz et al., 2018; Kung, 2005; Liu et al., 2018; Murthy et al., 2018a; Zhang et al., 2018).

Although the molecular architecture of mammalian MSCs is quite diverse, a common finding is the presence of large fenestrations within the wall of the pores (although absent in Piezo2) directly facing membrane lipids (above the constriction for Piezo1 and below for the other MSCs) (Figure 1).

It is worth considering whether lipid occupancy within lateral fenestrations might be a general mechanism for the modulation of MSCs gating/permeation (Brohawn et al., 2014a)(Figure 3A).

Whether or not different gating mechanisms are recruited for specific mechanical inputs is unknown. For instance, flow activation of TREK-1 or Piezo1 may be direct, possibly acting on the extracellular glycosylated loops, or alternatively might require the presence of an additional flow sensor (for instance the extracellular matrix or another transmembrane protein) present at the apical side of endothelial cells (Li et al., 2014; Ranade et al., 2014a; Wang et al., 2016).Both non-specialized cells (including epithelial cells or RBCs), as well as specialized cells responsible for mechanosensory transduction (including touch sensitive neurons, hair cells and baroreceptors) are equipped with a variety of MSCs characterized by a different ionic selectivity (hyperpolarizing K^+-selective or depolarizing cationic non-selective) and gating properties (high and low mechanical threshold). Moreover, the cortical cytoskeleton additionally greatly influences mechano-gating of ion channels (Cox et al., 2016; Lauritzen et al., 2005; Peyronnet et al., 2012; Retailleau et al., 2016)(Figure 6). For instance, when Piezo1 is activated in membrane blebs lacking cytoskeleton, gating occurs at lower pressure, as compared to classical cell-attached patch recordings in intact cells (Cox et al., 2016). More work will be required to better understand the mechanoprotection of MSCs by the cytoskeleton (Figure 6).

Over the years, additional ion channels were implicated in mechanosensory transduction, including MEC/DEG/ASICS and TRPs in lower organisms, as well as in mammals (Chalfie, 2009; Christensen and Corey, 2007; Lin et al., 2016; Walker et al., 2000; Yan et al., 2013). However, so far no clear evidence was provided demonstrating their intrinsic mechanosensitivity. Whether or not those additional players might be acting in parallel or downstream of *bonafide* MSCs needs to be investigated.

The recent structural, functional and physiological findings about MSCs have tremendously improved our understanding of cellular mechanotransduction and related disease states. However, multiple questions remain open and will certainly be the topic of intense research in the coming years. Among those questions: What is the structure of Piezo1 in the open state? Does Piezo1 modulate neighboring molecules (including other MSCs) through curvature? Does Piezo2 also flatten upon activation? What is the specific pathophysiological role of the TMEM63a,b,c isoforms? What is the structure of TMC1/2? Does TMC1/TMC2 form the entire pore of the hair cell transduction channel? What is the contribution of membrane lipids and other transmembrane proteins in the hair cell MET channel? What are the gating mechanisms of TMC1/TMC2? Which and how lipids affect MSCs gating? How phosphorylation/dephosphorylation regulates MSCs gating? How TMEM150c modulates MSCs inactivation? What is the physiological role of TMEM150c? Since various MSCs are expressed in the same cell types, how cells integrate different mechanical inputs? What regulates the balance between depolarizing and hyperpolarizing MSCs? Which MSCs channels are involved in mechanical

nociception? What are the MSCs and their regulators that remain to be discovered? Also, the pharmacology of MSCs is still in the early days, and identification of selective and potent molecules (activators or blockers) will undoubtedly be very useful for possible clinical applications.

Figure legends:

Figure 1: Structures of mammalian MSCs. The ionic pathways are shown in red, zoomed lateral fenestrations in yellow (anticipated to be filled with lipids) and residues forming constrictions in orange (zooms are not at the same scale). (**A**) hTRAAK with TM4 down (in blue and dashed magenta line) (PDB 4WFF) or up (in green and no dash magenta line)(PDB 4WFE). Central zoom: a 10 carbon long lipid chain (in yellow) is shown in the TRAAK fenestration zoom (circled in yellow), when TM4 is down (dashed magenta line). The selectivity filter (that controls permeability and presumably acts as an activation gate for TREK/TRAAK K_{2P} channels) is shown in orange. (**B**) mPiezo1 in the closed state (PDB 6B3R). (**C**) AtOSCA1.2 in the closed state (PDB 6IJZ). (**D**) Structural model of hTMC1 (closed state), based on TMEM16A structure (Pan et al., 2018). All channels are at the same scale. For hTMC1 Tyr 455, Phe 457, Glu 523 and Arg 526 are predicted to form an upper constriction. In B-D zooms, structures were rotated to better visualize lateral cavities.

Figure 2: Gating properties of MSCs. (**A**) Gating curves of TREK/TRAAK K_{2P} channels (in red), Piezo1 (in magenta) and MscL (in blue). (**B**) Upward movement of TM4 (down in blue and up in green) is associated with a modest increase in the cross-sectional area of TRAAK (2.7 nm^2) (Brohawn et al., 2014a), while a Large expansion of MscL (20 nm^2) occurs upon channel opening (PDB 4y7k and PDB 4y7j, for closed an open states, respectively))(Perozo et al., 2002). Channels are at scale (bottom views) and TRAAK TM4 is highlighted in dark blue or light green. (**C**) Membrane stretch (in red) induces an expansion of the inner part of TREK-2 (arrow)(Aryal et al., 2017). The Z axis (in Angstrom) is centered on the middle of the bilayer. (**D**) MD simulation of the transbilayer pressure profile of an ideal membrane in which TREK-2 is inserted (Aryal et al., 2017). Arrows indicate major changes induced by stretch (P: -50 mm Hg in red).

Figure 3: Gating models for TREK/TRAAK K_{2P} channels. (**A**) Blocking lipids (in yellow) insert in the lateral fenestrations when TM4 is down and prevent K^+ permeation (Brohawn et al., 2014a). Upon stretch TM4 segments move upward, seal lateral fenestrations and prevent insertion of lipids, thus allowing K^+ efflux through the selectivity filter (Brohawn et al., 2014a). (**B**) ML335/ML402 are small molecule TREK-1 activators (shown as purple spheres) binding to a cryptic selectivity filter site, stabilizing the C-type gate "leak mode", by reducing mobility (illustrated by curved arcs) of selectivity filter elements (Lolicato et al., 2017). (**C**) Activated cytosolic Ct (acidic pH_i causing protonation of the

glutamate residue E306, shown in green) is in interaction with the membrane. On the contrary, phosphorylation by protein kinase A or C at S300/S333 in the Ct (shown in red) prevents TREK-1 activation. The TREK-1 Ct relays mechanical, thermal and acidic modulations to the filter C-type gate through transmembrane helix TM4 and pore helix 1 (shown by a dashed black arrow).

Figure 4: Piezo1 curvature and mechanosensitivity. (**A**) Piezo1 trimeric (only two monomers are shown) structure is curved. The blades formed by 9 helices repeats (dark blue) are shown in light blue. Each repeat forming the blades comprises 4 TMs (not shown). A: anchor; CTD: carboxy terminal domain; CED: extracellular carboxy terminal domain; IH: inner helix. Lipids present within Piezo1 are shown in gray. (**B**) mPiezo1 deforms the membrane in a dome shape (side view). (**C**) Triskelion structure of mPiezo1 seen from top. (**D**) Flattening of Piezo1 in response to an increase in membrane tension, anticipated to cause a 120 nm^2 increase of the projected in-plane channel area (ΔA).

Figure 5: **OSCA and predicted TMC1 structures**. (**A**) Transmembrane topology of TMEM63/OSCA. (**B**) Ionic pathways (in brown) and anchoring of IL2H2-IL2H3 loop (in purple) into the lipid bilayer. (**C**) Predicted TMC1 and PCDH15 transmembrane topologies. The C terminal domain of PCDH15 (cis-dimeric architecture) interacts with the N terminus of TMC1. (**D**) Positive deflection of the hair cell bundle at the apical side activates the MET channel. Force is transmitted to TMC1/TMC2 through the tip link made of PCDH15 and CDH23. The MET channel is located at the top of the lower stereocilia that contain actin bundles. (**E**) Cysteine mutants affecting channel activity (no current or smaller current amplitude) or altered selectivity in hTMC1. The Beethoven mutation site Met 418 is highlighted in magenta.

Figure 6: **Mechanoprotection of MSCs**. (**A**) When the actin cross-linking protein filamin A is present the cortical actin cytoskeleton is stiff, membrane is locally curved and tension reaching the channel attenuated. (**B**) Increased MSC opening when the cytoskeleton is disrupted (deletion of filamin A in this case)(Sharif Naeini et al., 2009). The radius of membrane curvature (estimated by a dahed circle) is enhanced upon deletion of the actin cross-linking protein filamin A.

Key Table: Summary of the main functional properties of the mammalian MSCs. Ionic selectivity (either K^+-selective or cationic non-selective), effect on membrane potential (hyperpolarization or depolarization), gating by force-from-lipid or by a tether, single channel conductance (in pS), mechanical threshold, inactivation/adaptation, main tissue expression, viability of constitutive knock-out, main physiological function and associated genetic diseases are indicated.

Acknowledgements: We are grateful to Dr. Jeffrey Holt and Dr. David Corey for sharing with us the hTMC1 structural model. We thank the Fondation pour la Recherche Médicale, the Agence Nationale de la Recherche and the Human Frontier Science Program for funding this work. We thank F. Aguila for expert graphical help. We are grateful to Dr. Steve Brohawn, Dr. David Corey, Dr. Jeffrey Holt, Dr. Boris Martinac, Dr. Daniel Minor, Dr. Ardem Patapoutian and Dr. Stephen Tucker for valuable comments on this manuscript. This review is dedicated to the memory of the late Pr. Paul M. Vanhoutte.

References:

Albuisson, J., Murthy, S.E., Bandell, M., Coste, B., Louis-Dit-Picard, H., Mathur, J., Feneant-Thibault, M., Tertian, G., de Jaureguiberry, J.P., Syfuss, P.Y.*, et al.* (2013). Dehydrated hereditary stomatocytosis linked to gain-of-function mutations in mechanically activated PIEZO1 ion channels. Nat Commun *4*, 1884.

Alloui, A., Zimmermann, K., Mamet, J., Duprat, F., Noel, J., Chemin, J., Guy, N., Blondeau, N., Voilley, N., Rubat-Coudert, C.*, et al.* (2006). TREK-1, a K+ channel involved in polymodal pain perception. EMBO J *25*, 2368-2376.

Anderson, E.O., Schneider, E.R., Matson, J.D., Gracheva, E.O., and Bagriantsev, S.N. (2018). TMEM150C/Tentonin3 Is a Regulator of Mechano-gated Ion Channels. Cell Rep *23*, 701-708.

Aryal, P., Jarerattanachat, V., Clausen, M.V., Schewe, M., McClenaghan, C., Argent, L., Conrad, L.J., Dong, Y.Y., Pike, A.C.W., Carpenter, E.P.*, et al.* (2017). Bilayer-Mediated Structural Transitions Control Mechanosensitivity of the TREK-2 K2P Channel. Structure *25*, 708-718 e702.

Bae, C., Gnanasambandam, R., Nicolai, C., Sachs, F., and Gottlieb, P.A. (2013). Xerocytosis is caused by mutations that alter the kinetics of the mechanosensitive channel PIEZO1. Proc Natl Acad Sci U S A *110*, E1162-1168.

Bagriantsev, S.N., Clark, K.A., and Minor, D.L., Jr. (2012). Metabolic and thermal stimuli control K(2P)2.1 (TREK-1) through modular sensory and gating domains. EMBO J *31*, 3297-3308.

Bagriantsev, S.N., Peyronnet, R., Clark, K.A., Honore, E., and Minor, D.L., Jr. (2011). Multiple modalities converge on a common gate to control K2P channel function. EMBO J *30*, 3594-3606.

Ballesteros, A., Fenollar-Ferrer, C., and Swartz, K.J. (2018). Structural relationship between the putative hair cell mechanotransduction channel TMC1 and TMEM16 proteins. Elife *7*.

Bauer, C.K., Calligari, P., Radio, F.C., Caputo, V., Dentici, M.L., Falah, N., High, F., Pantaleoni, F., Barresi, S., Ciolfi, A.*, et al.* (2018). Mutations in KCNK4 that Affect Gating Cause a Recognizable Neurodevelopmental Syndrome. Am J Hum Genet *103*, 621-630.

Beurg, M., Cui, R., Goldring, A.C., Ebrahim, S., Fettiplace, R., and Kachar, B. (2018). Variable number of TMC1-dependent mechanotransducer channels underlie tonotopic conductance gradients in the cochlea. Nat Commun *9*, 2185.

Brohawn, S.G., Campbell, E.B., and MacKinnon, R. (2014a). Physical mechanism for gating and mechanosensitivity of the human TRAAK K+ channel. Nature *516*, 126-130.

Brohawn, S.G., del Marmol, J., and MacKinnon, R. (2012). Crystal structure of the human K2P TRAAK, a lipid- and mechano-sensitive K^+ ion channel. Science *335*, 436-441.

Brohawn, S.G., Su, Z., and MacKinnon, R. (2014b). Mechanosensitivity is mediated directly by the lipid membrane in TRAAK and TREK1 K+ channels. Proc Natl Acad Sci U S A *111*, 3614-3619.

Cahalan, S.M., Lukacs, V., Ranade, S.S., Chien, S., Bandell, M., and Patapoutian, A. (2015). Piezo1 links mechanical forces to red blood cell volume. Elife *4*.

Chalfie, M. (2009). Neurosensory mechanotransduction. Nat Rev Mol Cell Biol *10*, 44-52.

Chen, X., Wanggou, S., Bodalia, A., Zhu, M., Dong, W., Fan, J.J., Yin, W.C., Min, H.K., Hu, M., Draghici, D.*, et al.* (2018). A Feedforward Mechanism Mediated by Mechanosensitive Ion Channel PIEZO1 and Tissue Mechanics Promotes Glioma Aggression. Neuron *100*, 799-815 e797.

Christensen, A.P., and Corey, D.P. (2007). TRP channels in mechanosensation: direct or indirect activation? Nat Rev Neurosci *8*, 510-521.

Clausen, M.V., Jarerattanachat, V., Carpenter, E.P., Sansom, M.S.P., and Tucker, S.J. (2017). Asymmetric mechanosensitivity in a eukaryotic ion channel. Proc Natl Acad Sci U S A *114*, E8343-E8351.

Corey, D.P., and Hudspeth, A.J. (1979). Ionic basis of the receptor potential in a vertebrate hair cell. Nature *281*, 675-677.

Coste, B., Houge, G., Murray, M.F., Stitziel, N., Bandell, M., Giovanni, M.A., Philippakis, A., Hoischen, A., Riemer, G., Steen, U.*, et al.* (2013). Gain-of-function mutations in the mechanically activated ion channel PIEZO2 cause a subtype of Distal Arthrogryposis. Proc Natl Acad Sci U S A *110*, 4667-4672.

Coste, B., Mathur, J., Schmidt, M., Earley, T.J., Ranade, S., Petrus, M.J., Dubin, A.E., and Patapoutian, A. (2010). Piezo1 and Piezo2 are essential components of distinct mechanically activated cation channels. Science *330*, 55-60.

Cox, C.D., Bae, C., Ziegler, L., Hartley, S., Nikolova-Krstevski, V., Rohde, P.R., Ng, C.A., Sachs, F., Gottlieb, P.A., and Martinac, B. (2016). Removal of the mechanoprotective influence of the cytoskeleton reveals PIEZO1 is gated by bilayer tension. Nat Commun *7*, 10366.

Delle Vedove, A., Storbeck, M., Heller, R., Holker, I., Hebbar, M., Shukla, A., Magnusson, O., Cirak, S., Girisha, K.M., O'Driscoll, M.*, et al.* (2016). Biallelic Loss of Proprioception-Related PIEZO2 Causes Muscular Atrophy with Perinatal Respiratory Distress, Arthrogryposis, and Scoliosis. Am J Hum Genet *99*, 1406-1408.

Delmas, P., and Coste, B. (2013). Mechano-gated ion channels in sensory systems. Cell *155*, 278-284.

Dionne, G., Qiu, X., Rapp, M., Liang, X., Zhao, B., Peng, G., Katsamba, P.S., Ahlsen, G., Rubinstein, R., Potter, C.S.*, et al.* (2018). Mechanotransduction by PCDH15 Relies on a Novel cis-Dimeric Architecture. Neuron *99*, 480-492 e485.

Dong, Y.Y., Pike, A.C., Mackenzie, A., McClenaghan, C., Aryal, P., Dong, L., Quigley, A., Grieben, M., Goubin, S., Mukhopadhyay, S.*, et al.* (2015). K2P channel gating mechanisms revealed by structures of TREK-2 and a complex with Prozac. Science *347*, 1256-1259.

Dubin, A.E., Murthy, S., Lewis, A.H., Brosse, L., Cahalan, S.M., Grandl, J., Coste, B., and Patapoutian, A. (2017). Endogenous Piezo1 Can Confound Mechanically Activated Channel Identification and Characterization. Neuron *94*, 266-270 e263.

Fettiplace, R. (2016). Is TMC1 the Hair Cell Mechanotransducer Channel? Biophys J *111*, 3-9.

Ge, J., Elferich, J., Goehring, A., Zhao, H., Schuck, P., and Gouaux, E. (2018). Structure of mouse protocadherin 15 of the stereocilia tip link in complex with LHFPL5. Elife *7*.

Ge, J., Li, W., Zhao, Q., Li, N., Chen, M., Zhi, P., Li, R., Gao, N., Xiao, B., and Yang, M. (2015). Architecture of the mammalian mechanosensitive Piezo1 channel. Nature *527*, 64-69.

Gillespie, P.G., and Muller, U. (2009). Mechanotransduction by hair cells: models, molecules, and mechanisms. Cell *139*, 33-44.

Guo, Y.R., and MacKinnon, R. (2017). Structure-based membrane dome mechanism for Piezo mechanosensitivity. Elife *6*.

Haliloglu, G., Becker, K., Temucin, C., Talim, B., Kucuksahin, N., Pergande, M., Motameny, S., Nurnberg, P., Aydingoz, U., Topaloglu, H.*, et al.* (2017). Recessive PIEZO2 stop mutation causes distal arthrogryposis with distal muscle weakness, scoliosis and proprioception defects. J Hum Genet *62*, 497-501.

Haselwandter, C.A., and MacKinnon, R. (2018). Piezo's membrane footprint and its contribution to mechanosensitivity. Elife *7*.

Hong, G.S., Lee, B., Wee, J., Chun, H., Kim, H., Jung, J., Cha, J.Y., Riew, T.R., Kim, G.H., Kim, I.B.*, et al.* (2016). Tentonin 3/TMEM150c Confers Distinct Mechanosensitive Currents in Dorsal-Root Ganglion Neurons with Proprioceptive Function. Neuron *91*, 107-118.

Honoré, E. (2007). The neuronal background K2P channels: focus on TREK-1. Nature reviews neuroscience *8*, 251-261.

Honoré, E., Patel, A.J., Chemin, J., Suchyna, T., and Sachs, F. (2006). Desensitization of mechano-gated K2P channels. Proc Natl Acad Sci U S A *103*, 6859-6864.

Hudspeth, A.J., Choe, Y., Mehta, A.D., and Martin, P. (2000). Putting ion channels to work: mechanoelectrical transduction, adaptation, and amplification by hair cells. Proc Natl Acad Sci U S A *97*, 11765-11772.

Jojoa-Cruz, S., Saotome, K., Murthy, S.E., Tsui, C.C.A., Sansom, M.S., Patapoutian, A., and Ward, A.B. (2018). Cryo-EM structure of the mechanically activated ion channel OSCA1.2. Elife *7*.

Kawashima, Y., Geleoc, G.S., Kurima, K., Labay, V., Lelli, A., Asai, Y., Makishima, T., Wu, D.K., Della Santina, C.C., Holt, J.R.*, et al.* (2011). Mechanotransduction in mouse inner ear hair cells requires transmembrane channel-like genes. J Clin Invest *121*, 4796-4809.

Kung, C. (2005). A possible unifying principle for mechanosensation. Nature *436*, 647-654.

Lauritzen, I., Chemin, J., Honoré, E., Jodar, M., Guy, N., Lazdunski, M., and Jane Patel, A. (2005). Cross-talk between the mechano-gated K2P channel TREK-1 and the actin cytoskeleton. EMBO Rep *6*, 642-648.

Lewis, A.H., and Grandl, J. (2015). Mechanical sensitivity of Piezo1 ion channels can be tuned by cellular membrane tension. Elife *4*.

Li, J., Hou, B., Tumova, S., Muraki, K., Bruns, A., Ludlow, M.J., Sedo, A., Hyman, A.J., McKeown, L., Young, R.S.*, et al.* (2014). Piezo1 integration of vascular architecture with physiological force. Nature *515*, 279-282.

Li, X., Yu, X., Chen, X., Liu, Z., Wang, G., Li, C., Wong, E.Y.M., Sham, M.H., Tang, J., He, J.*, et al.* (2019). Localization of TMC1 and LHFPL5 in auditory hair cells in neonatal and adult mice. FASEB J, fj201802155RR.

Liang, X., and Howard, J. (2018). Structural Biology: Piezo Senses Tension through Curvature. Curr Biol *28*, R357-R359.

Lin, S.H., Cheng, Y.R., Banks, R.W., Min, M.Y., Bewick, G.S., and Chen, C.C. (2016). Evidence for the involvement of ASIC3 in sensory mechanotransduction in proprioceptors. Nat Commun *7*, 11460.

Lin, Y.C., Guo, Y.R., Miyagi, A., Levring, J., MacKinnon, R., and Scheuring, S. (2019). Force-induced conformational changes in PIEZO1. Nature.

Liu, X., Wang, J., and Sun, L. (2018). Structure of the hyperosmolality-gated calcium-permeable channel OSCA1.2. Nat Commun *9*, 5060.

Lolicato, M., Arrigoni, C., Mori, T., Sekioka, Y., Bryant, C., Clark, K.A., and Minor, D.L., Jr. (2017). K2P2.1 (TREK-1)-activator complexes reveal a cryptic selectivity filter binding site. Nature *547*, 364-368.

Lolicato, M., Riegelhaupt, P.M., Arrigoni, C., Clark, K.A., and Minor, D.L., Jr. (2014). Transmembrane helix straightening and buckling underlies activation of mechanosensitive and thermosensitive K(2P) channels. Neuron *84*, 1198-1212.

Lukacs, V., Mathur, J., Mao, R., Bayrak-Toydemir, P., Procter, M., Cahalan, S.M., Kim, H.J., Bandell, M., Longo, N., Day, R.W.*, et al.* (2015). Impaired PIEZO1 function in patients with a novel autosomal recessive congenital lymphatic dysplasia. Nat Commun *6*, 8329.

Ma, S., Cahalan, S., LaMonte, G., Grubaugh, N.D., Zeng, W., Murthy, S.E., Paytas, E., Gamini, R., Lukacs, V., Whitwam, T.*, et al.* (2018). Common PIEZO1 Allele in African Populations Causes RBC Dehydration and Attenuates Plasmodium Infection. Cell *173*, 443-455 e412.

Maeda, R., Kindt, K.S., Mo, W., Morgan, C.P., Erickson, T., Zhao, H., Clemens-Grisham, R., Barr-Gillespie, P.G., and Nicolson, T. (2014). Tip-link protein protocadherin 15 interacts with transmembrane channel-like proteins TMC1 and TMC2. Proc Natl Acad Sci U S A *111*, 12907-12912.

Maingret, F., Patel, A.J., Lesage, F., Lazdunski, M., and Honoré, E. (2000). Lysophospholipids open the two P domain mechano-gated K^+ channels TREK-1 and TRAAK. J Biol Chem *275*, 10128-10133.

Maity, K., Heumann, J.M., McGrath, A.P., Kopcho, N.J., Hsu, P.K., Lee, C.W., Mapes, J.H., Garza, D., Krishnan, S., Morgan, G.P.*, et al.* (2019). Cryo-EM structure of OSCA1.2 from Oryza sativa elucidates the mechanical basis of potential membrane hyperosmolality gating. Proc Natl Acad Sci U S A *116*, 14309-14318.

Maksimovic, S., Nakatani, M., Baba, Y., Nelson, A.M., Marshall, K.L., Wellnitz, S.A., Firozi, P., Woo, S.H., Ranade, S., Patapoutian, A.*, et al.* (2014). Epidermal Merkel cells are mechanosensory cells that tune mammalian touch receptors. Nature *509*, 617-621.

Martinac, B., Adler, J., and Kung, C. (1990). Mechanosensitive ion channels of *E. Coli* activated by amphipaths. Nature *348*, 261-263.

Martinac, B., Bavi, N., Ridone, P., Nikolaev, Y.A., Martinac, A.D., Nakayama, Y., Rohde, P.R., and Bavi, O. (2018). Tuning ion channel mechanosensitivity by asymmetry of the transbilayer pressure profile. Biophys Rev *10*, 1377-1384.

McClenaghan, C., Schewe, M., Aryal, P., Carpenter, E.P., Baukrowitz, T., and Tucker, S.J. (2016). Polymodal activation of the TREK-2 K2P channel produces structurally distinct open states. J Gen Physiol *147*, 497-505.

Murthy, S.E., Dubin, A.E., and Patapoutian, A. (2017). Piezos thrive under pressure: mechanically activated ion channels in health and disease. Nat Rev Mol Cell Biol *18*, 771-783.

Murthy, S.E., Dubin, A.E., Whitwam, T., Jojoa-Cruz, S., Cahalan, S.M., Mousavi, S.A.R., Ward, A.B., and Patapoutian, A. (2018a). OSCA/TMEM63 are an Evolutionarily Conserved Family of Mechanically Activated Ion Channels. Elife *7*.

Murthy, S.E., Loud, M.C., Daou, I., Marshall, K.L., Schwaller, F., Kuhnemund, J., Francisco, A.G., Keenan, W.T., Dubin, A.E., Lewin, G.R.*, et al.* (2018b). The mechanosensitive ion channel Piezo2 mediates sensitivity to mechanical pain in mice. Sci Transl Med *10*.

Nist-Lund, C.A., Pan, B., Patterson, A., Asai, Y., Chen, T., Zhou, W., Zhu, H., Romero, S., Resnik, J., Polley, D.B.*, et al.* (2019). Improved TMC1 gene therapy restores hearing and balance in mice with genetic inner ear disorders. Nat Commun *10*, 236.

Noel, J., Zimmermann, K., Busserolles, J., Deval, E., Alloui, A., Diochot, S., Guy, N., Borsotto, M., Reeh, P., Eschalier, A.*, et al.* (2009). The mechano-activated K+ channels TRAAK and TREK-1 control both warm and cold perception. EMBO J *28*, 1308-1318.

Nonomura, K., Lukacs, V., Sweet, D.T., Goddard, L.M., Kanie, A., Whitwam, T., Ranade, S.S., Fujimori, T., Kahn, M.L., and Patapoutian, A. (2018). Mechanically activated ion channel PIEZO1 is required for lymphatic valve formation. Proc Natl Acad Sci U S A *115*, 12817-12822.

Nonomura, K., Woo, S.H., Chang, R.B., Gillich, A., Qiu, Z., Francisco, A.G., Ranade, S.S., Liberles, S.D., and Patapoutian, A. (2017). Piezo2 senses airway stretch and mediates lung inflation-induced apnoea. Nature *541*, 176-181.

Pan, B., Akyuz, N., Liu, X.P., Asai, Y., Nist-Lund, C., Kurima, K., Derfler, B.H., Gyorgy, B., Limapichat, W., Walujkar, S.*, et al.* (2018). TMC1 Forms the Pore of Mechanosensory Transduction Channels in Vertebrate Inner Ear Hair Cells. Neuron *99*, 736-753 e736.

Pan, B., Geleoc, G.S., Asai, Y., Horwitz, G.C., Kurima, K., Ishikawa, K., Kawashima, Y., Griffith, A.J., and Holt, J.R. (2013). TMC1 and TMC2 are components of the mechanotransduction channel in hair cells of the mammalian inner ear. Neuron *79*, 504-515.

Perozo, E., Cortes, D.M., Sompornpisut, P., Kloda, A., and Martinac, B. (2002). Open channel structure of MscL and the gating mechanism of mechanosensitive channels. Nature *418*, 942-948.

Peyronnet, R., Sharif-Naeini, R., Folgering, J.H., Arhatte, M., Jodar, M., El Boustany, C., Gallian, C., Tauc, M., Duranton, C., Rubera, I.*, et al.* (2012). Mechanoprotection by Polycystins against Apoptosis Is Mediated through the Opening of Stretch-Activated K(2P) Channels. Cell Rep *1*, 241-250.

Poole, K., Herget, R., Lapatsina, L., Ngo, H.D., and Lewin, G.R. (2014). Tuning Piezo ion channels to detect molecular-scale movements relevant for fine touch. Nat Commun *5*, 3520.

Qi, Y., Andolfi, L., Frattini, F., Mayer, F., Lazzarino, M., and Hu, J. (2015). Membrane stiffening by STOML3 facilitates mechanosensation in sensory neurons. Nat Commun *6*, 8512.

Qiu, X., and Muller, U. (2018). Mechanically Gated Ion Channels in Mammalian Hair Cells. Front Cell Neurosci *12*, 100.
Ranade, S.S., Qiu, Z., Woo, S.H., Hur, S.S., Murthy, S.E., Cahalan, S.M., Xu, J., Mathur, J., Bandell, M., Coste, B.*, et al.* (2014a). Piezo1, a mechanically activated ion channel, is required for vascular development in mice. Proc Natl Acad Sci U S A *111*, 10347-10352.
Ranade, S.S., Woo, S.H., Dubin, A.E., Moshourab, R.A., Wetzel, C., Petrus, M., Mathur, J., Begay, V., Coste, B., Mainquist, J.*, et al.* (2014b). Piezo2 is the major transducer of mechanical forces for touch sensation in mice. Nature *516*, 121-125.
Retailleau, K., Arhatte, M., Demolombe, S., Peyronnet, R., Baudrie, V., Jodar, M., Bourreau, J., Henrion, D., Offermanns, S., Nakamura, F.*, et al.* (2016). Arterial Myogenic Activation through Smooth Muscle Filamin A. Cell Rep *14*, 2050-2058.
Retailleau, K., Duprat, F., Arhatte, M., Ranade, S.S., Peyronnet, R., Martins, J.R., Jodar, M., Moro, C., Offermanns, S., Feng, Y.*, et al.* (2015). Piezo1 in Smooth Muscle Cells Is Involved in Hypertension-Dependent Arterial Remodeling. Cell Rep *13*, 1161-1171.
Richardson, G.P., de Monvel, J.B., and Petit, C. (2011). How the genetics of deafness illuminates auditory physiology. Annu Rev Physiol *73*, 311-334.
Rode, B., Shi, J., Endesh, N., Drinkhill, M.J., Webster, P.J., Lotteau, S.J., Bailey, M.A., Yuldasheva, N.Y., Ludlow, M.J., Cubbon, R.M.*, et al.* (2017). Piezo1 channels sense whole body physical activity to reset cardiovascular homeostasis and enhance performance. Nat Commun *8*, 350.
Romac, J.M., Shahid, R.A., Swain, S.M., Vigna, S.R., and Liddle, R.A. (2018). Piezo1 is a mechanically activated ion channel and mediates pressure induced pancreatitis. Nat Commun *9*, 1715.
Romero, L.O., Massey, A.E., Mata-Daboin, A.D., Sierra-Valdez, F.J., Chauhan, S.C., Cordero-Morales, J.F., and Vasquez, V. (2019). Dietary fatty acids fine-tune Piezo1 mechanical response. Nat Commun *10*, 1200.
Royal, P., Andres-Bilbe, A., Avalos Prado, P., Verkest, C., Wdziekonski, B., Schaub, S., Baron, A., Lesage, F., Gasull, X., Levitz, J.*, et al.* (2019). Migraine-Associated TRESK Mutations Increase Neuronal Excitability through Alternative Translation Initiation and Inhibition of TREK. Neuron *101*, 232-245 e236.
Sachs, F., and Morris, C.E. (1998). Mechanosensitive ion channels in nonspecialized cells. Rev Physiol Biochem Pharmacol *132*, 1-77.
Saotome, K., Murthy, S.E., Kefauver, J.M., Whitwam, T., Patapoutian, A., and Ward, A.B. (2018). Structure of the mechanically activated ion channel Piezo1. Nature *554*, 481-486.
Schewe, M., Nematian-Ardestani, E., Sun, H., Musinszki, M., Cordeiro, S., Bucci, G., de Groot, B.L., Tucker, S.J., Rapedius, M., and Baukrowitz, T. (2016). A Non-canonical Voltage-Sensing Mechanism Controls Gating in K2P K(+) Channels. Cell *164*, 937-949.
Sharif Naeini, R., Folgering, J., Bichet, D., Duprat, F., Lauritzen, I., Arhatte, M., Jodar, M., Dedman, A., Chatelain, F.C., Schulte, U.*, et al.* (2009). Polycystin-1 and -2 dosage regulates pressure sensing. Cell *139*, 587-596.
Shin, K.C., Park, H.J., Kim, J.G., Lee, I.H., Cho, H., Park, C., Sung, T.S., Koh, S.D., Park, S.W., and Bae, Y.M. (2019). The Piezo2 ion channel is mechanically activated by low-threshold positive pressure. Sci Rep *9*, 6446.
Sukharev, S.I., Blount, P., Martinac, B., Blattner, F.R., and Kung, C. (1994). A large-conductance mechanosensitive channel in *E. coli* encoded by mscL alone. Nature *368*, 265-268.
Syeda, R., Florendo, M.N., Cox, C.D., Kefauver, J.M., Santos, J.S., Martinac, B., and Patapoutian, A. (2016). Piezo1 Channels Are Inherently Mechanosensitive. Cell Rep *17*, 1739-1746.
Syeda, R., Xu, J., Dubin, A.E., Coste, B., Mathur, J., Huynh, T., Matzen, J., Lao, J., Tully, D.C., Engels, I.H.*, et al.* (2015). Chemical activation of the mechanotransduction channel Piezo1. Elife *4*.
Szczot, M., Liljencrantz, J., Ghitani, N., Barik, A., Lam, R., Thompson, J.H., Bharucha-Goebel, D., Saade, D., Necaise, A., Donkervoort, S.*, et al.* (2018). PIEZO2 mediates injury-induced tactile pain in mice and humans. Sci Transl Med *10*.
Walker, R.G., Willingham, A.T., and Zuker, C.S. (2000). A Drosophila mechanosensory transduction channel. Science *287*, 2229-2234.

Wang, L., Zhou, H., Zhang, M., Liu, W., Deng, T., Zhao, Q., Li, Y., Lei, J., Li, X., and Xiao, B. (2019). Structure and mechanogating of the mammalian tactile channel PIEZO2. Nature.

Wang, S., Chennupati, R., Kaur, H., Iring, A., Wettschureck, N., and Offermanns, S. (2016). Endothelial cation channel PIEZO1 controls blood pressure by mediating flow-induced ATP release. J Clin Invest *126*, 4527-4536.

Wetzel, C., Pifferi, S., Picci, C., Gok, C., Hoffmann, D., Bali, K.K., Lampe, A., Lapatsina, L., Fleischer, R., Smith, E.S.*, et al.* (2017). Small-molecule inhibition of STOML3 oligomerization reverses pathological mechanical hypersensitivity. Nat Neurosci *20*, 209-218.

Woo, S.H., Lukacs, V., de Nooij, J.C., Zaytseva, D., Criddle, C.R., Francisco, A., Jessell, T.M., Wilkinson, K.A., and Patapoutian, A. (2015). Piezo2 is the principal mechanotransduction channel for proprioception. Nat Neurosci *18*, 1756-1762.

Woo, S.H., Ranade, S., Weyer, A.D., Dubin, A.E., Baba, Y., Qiu, Z., Petrus, M., Miyamoto, T., Reddy, K., Lumpkin, E.A.*, et al.* (2014). Piezo2 is required for Merkel-cell mechanotransduction. Nature *509*, 622-626.

Wu, J., Lewis, A.H., and Grandl, J. (2017a). Touch, Tension, and Transduction - The Function and Regulation of Piezo Ion Channels. Trends Biochem Sci *42*, 57-71.

Wu, Z., Grillet, N., Zhao, B., Cunningham, C., Harkins-Perry, S., Coste, B., Ranade, S., Zebarjadi, N., Beurg, M., Fettiplace, R.*, et al.* (2017b). Mechanosensory hair cells express two molecularly distinct mechanotransduction channels. Nat Neurosci *20*, 24-33.

Yan, Z., Zhang, W., He, Y., Gorczyca, D., Xiang, Y., Cheng, L.E., Meltzer, S., Jan, L.Y., and Jan, Y.N. (2013). Drosophila NOMPC is a mechanotransduction channel subunit for gentle-touch sensation. Nature *493*, 221-225.

Yuan, F., Yang, H., Xue, Y., Kong, D., Ye, R., Li, C., Zhang, J., Theprungsirikul, L., Shrift, T., Krichilsky, B.*, et al.* (2014). OSCA1 mediates osmotic-stress-evoked Ca2+ increases vital for osmosensing in Arabidopsis. Nature *514*, 367-371.

Zarychanski, R., Schulz, V.P., Houston, B.L., Maksimova, Y., Houston, D.S., Smith, B., Rinehart, J., and Gallagher, P.G. (2012). Mutations in the mechanotransduction protein PIEZO1 are associated with hereditary xerocytosis. Blood *120*, 1908-1915.

Zeng, W.Z., Marshall, K.L., Min, S., Daou, I., Chapleau, M.W., Abboud, F.M., Liberles, S.D., and Patapoutian, A. (2018). PIEZOs mediate neuronal sensing of blood pressure and the baroreceptor reflex. Science *362*, 464-467.

Zhang, M., Wang, D., Kang, Y., Wu, J.X., Yao, F., Pan, C., Yan, Z., Song, C., and Chen, L. (2018). Structure of the mechanosensitive OSCA channels. Nat Struct Mol Biol *25*, 850-858.

Zhao, Q., Wu, K., Geng, J., Chi, S., Wang, Y., Zhi, P., Zhang, M., and Xiao, B. (2016). Ion Permeation and Mechanotransduction Mechanisms of Mechanosensitive Piezo Channels. Neuron *89*, 1248-1263.

Zhao, Q., Zhou, H., Chi, S., Wang, Y., Wang, J., Geng, J., Wu, K., Liu, W., Zhang, T., Dong, M.Q.*, et al.* (2018). Structure and mechanogating mechanism of the Piezo1 channel. Nature *554*, 487-492.

Zheng, W., Gracheva, E.O., and Bagriantsev, S.N. (2019). A hydrophobic gate in the inner pore helix is the major determinant of inactivation in mechanosensitive Piezo channels. Elife *8*.

Fig. 1

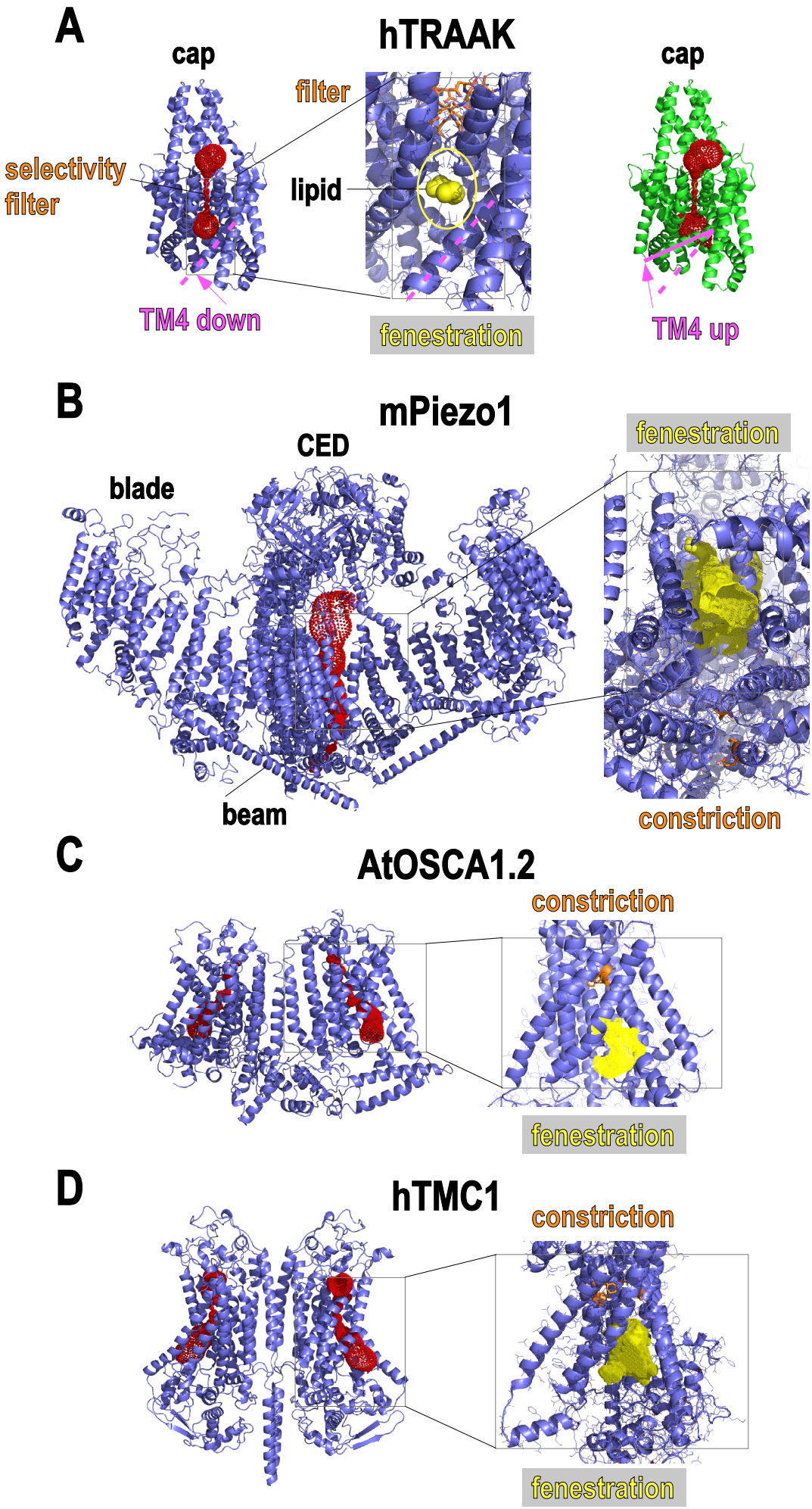
A
hTRAAK
cap
filter
selectivity filter
lipid
cap
TM4 down
fenestration
TM4 up
B
mPiezo1
CED
blade
fenestration
beam
constriction
C
AtOSCA1.2
constriction
fenestration
D
hTMC1
constriction
fenestration

Fig. 2

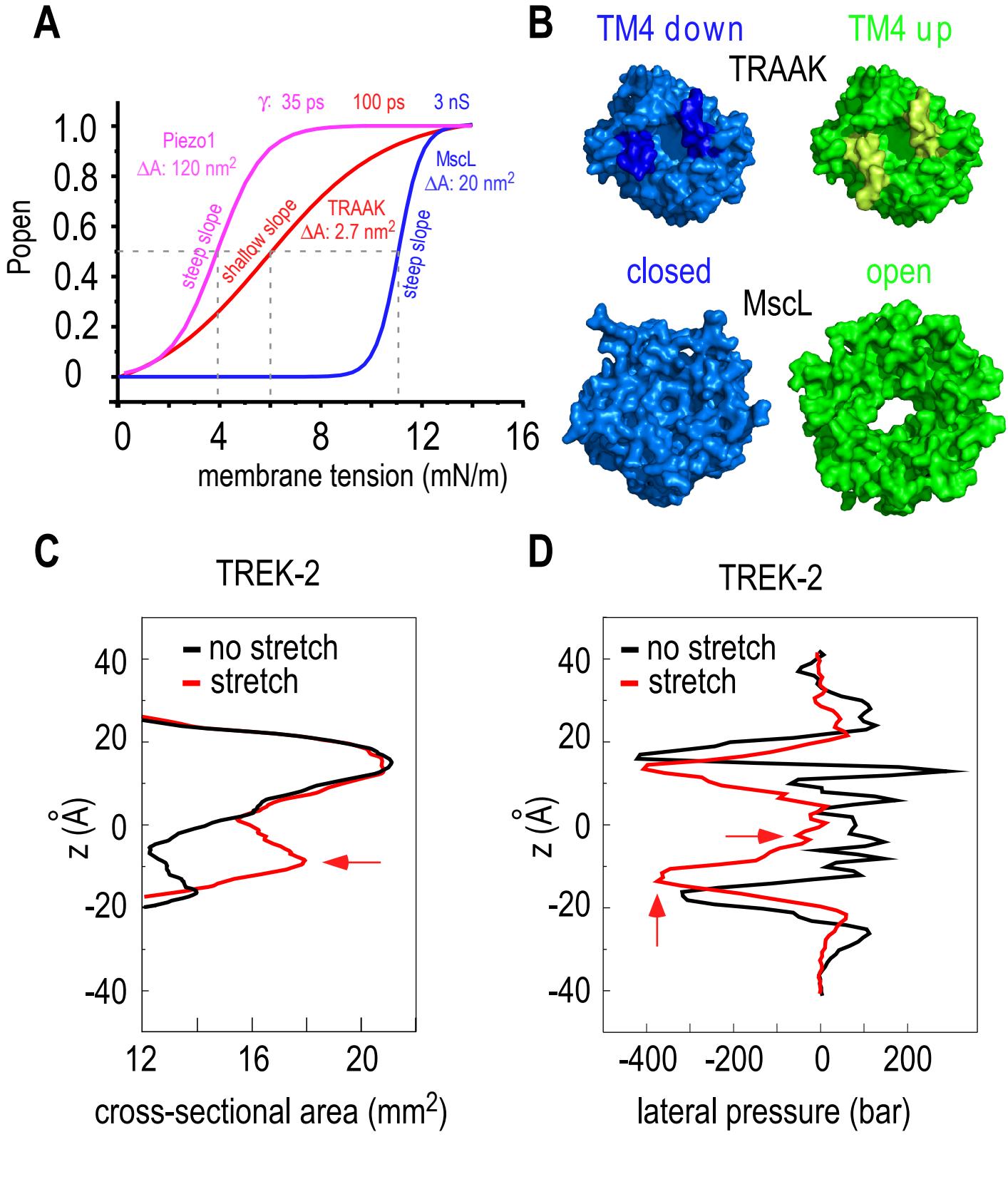
A
γ: 35 ps
100 ps
3 nS
Piezo1
ΔA: 120 nm²
MscL
ΔA: 20 nm²
TRAAK
ΔA: 2.7 nm²
steep slope
shallow slope
steep slope
Popen
1.0
0.8
0.6
0.4
0.2
0
0
4
8
12
16
membrane tension (mN/m)
B
TM4 down
TM4 up
TRAAK
closed
open
MscL
C
TREK-2
no stretch
stretch
40
20
0
-20
-40
z (Å)
12
16
20
cross-sectional area (mm²)
D
TREK-2
no stretch
stretch
40
20
0
-20
-40
z (Å)
-400
-200
0
200
lateral pressure (bar)

Fig. 3

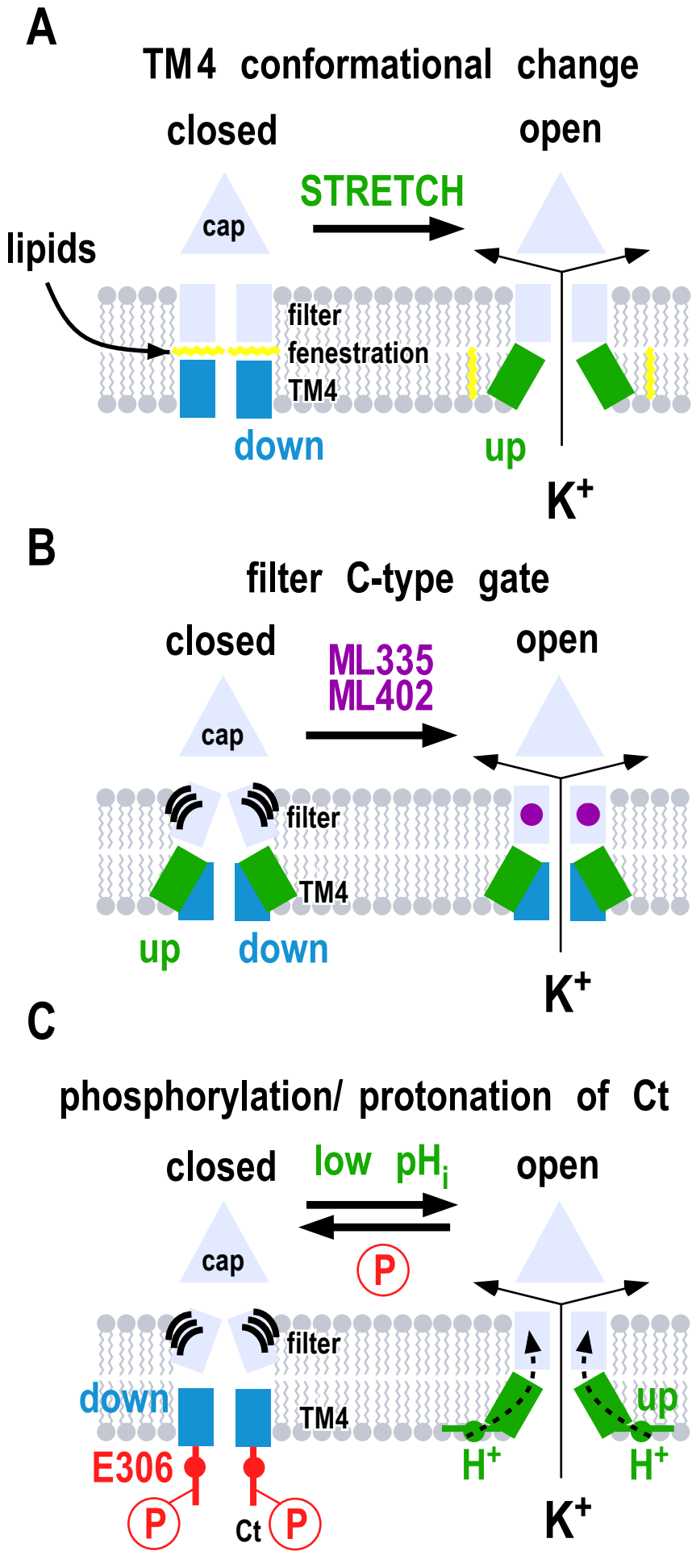
A
TM4 conformational change
closed
open
STRETCH
cap
lipids
filter
fenestration
TM4
down
up
K+
B
filter C-type gate
closed
open
ML335
ML402
cap
filter
TM4
up
down
K+
C
phosphorylation/ protonation of Ct
closed
low pHi
open
P
cap
filter
down
TM4
up
E306
H+
H+
P
Ct
P
K+

Fig. 4

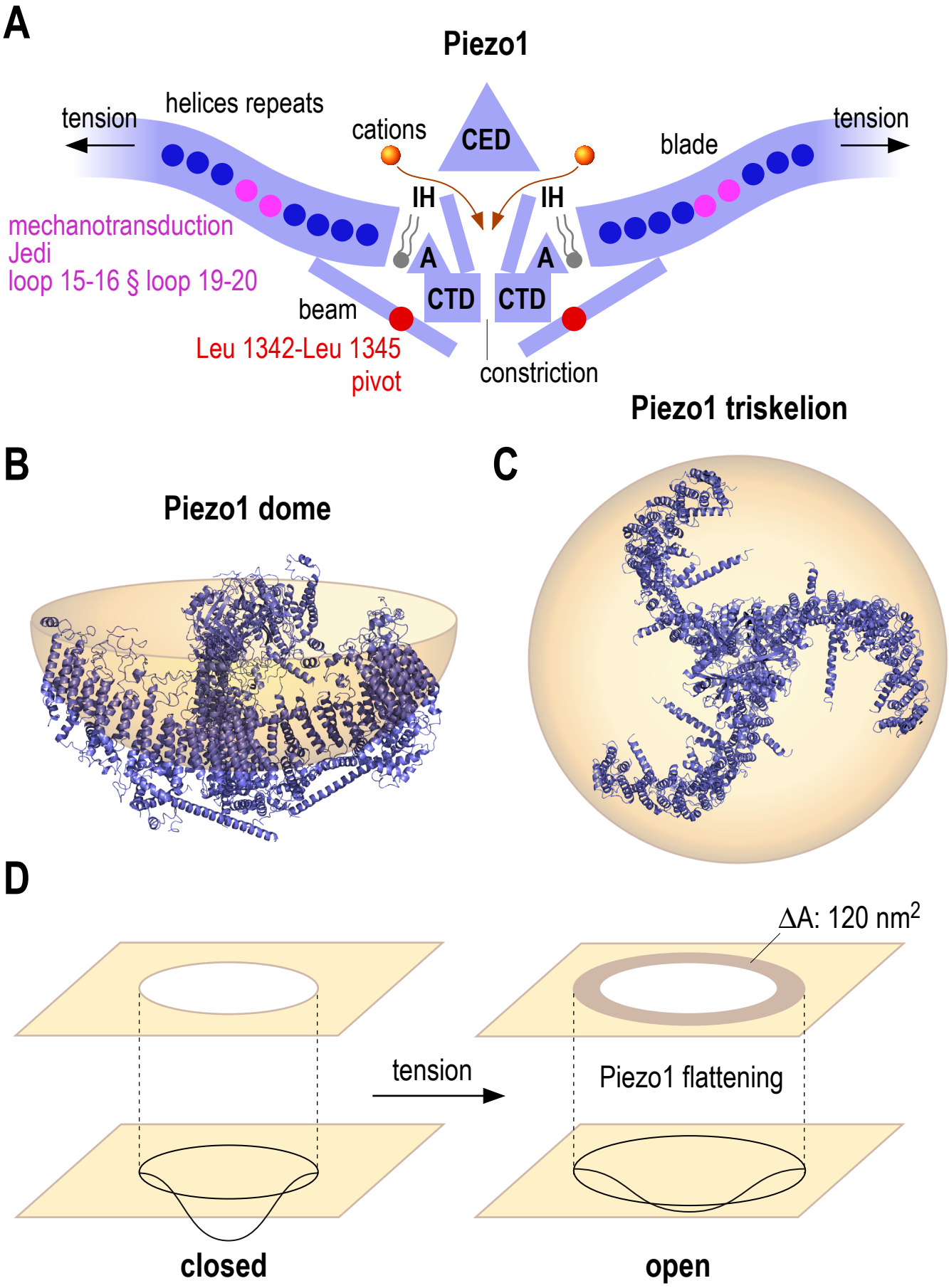
A
Piezo1
tension
helices repeats
cations
CED
blade
tension
IH
IH
mechanotransduction
Jedi
loop 15-16 § loop 19-20
A
A
CTD
CTD
beam
Leu 1342-Leu 1345
pivot
constriction
Piezo1 triskelion
B
Piezo1 dome
C
D
ΔA: 120 nm2
tension
Piezo1 flattening
closed
open

Fig. 5

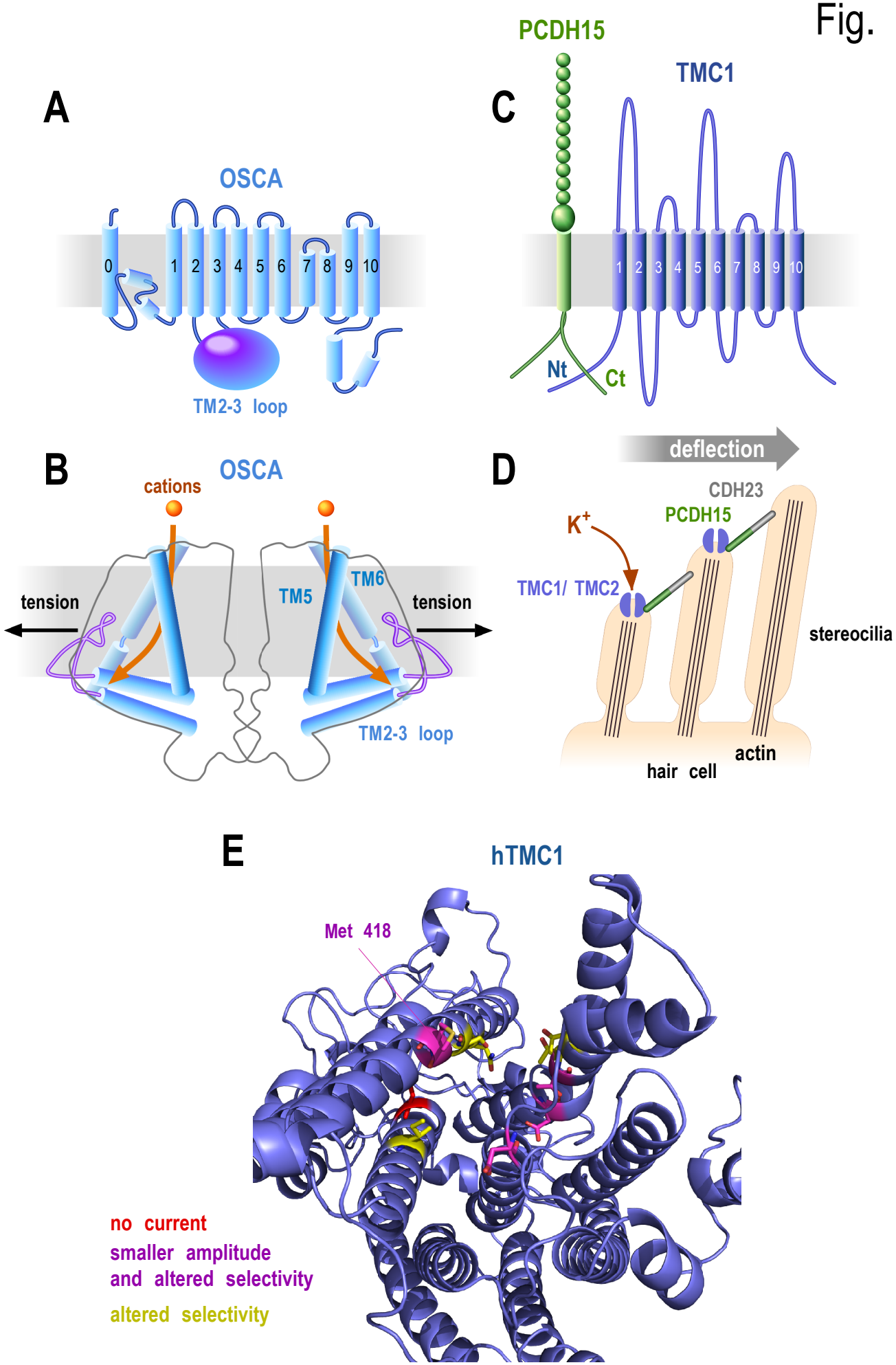
A
OSCA
0 1 2 3 4 5 6 7 8 9 10
TM2-3 loop
B
OSCA
cations
tension
TM5
TM6
tension
TM2-3 loop
C
PCDH15
TMC1
1 2 3 4 5 6 7 8 9 10
Nt
Ct
D
deflection
CDH23
PCDH15
K+
TMC1/ TMC2
stereocilia
actin
hair cell
E
hTMC1
Met 418
no current
smaller amplitude
and altered selectivity
altered selectivity

Fig. 6

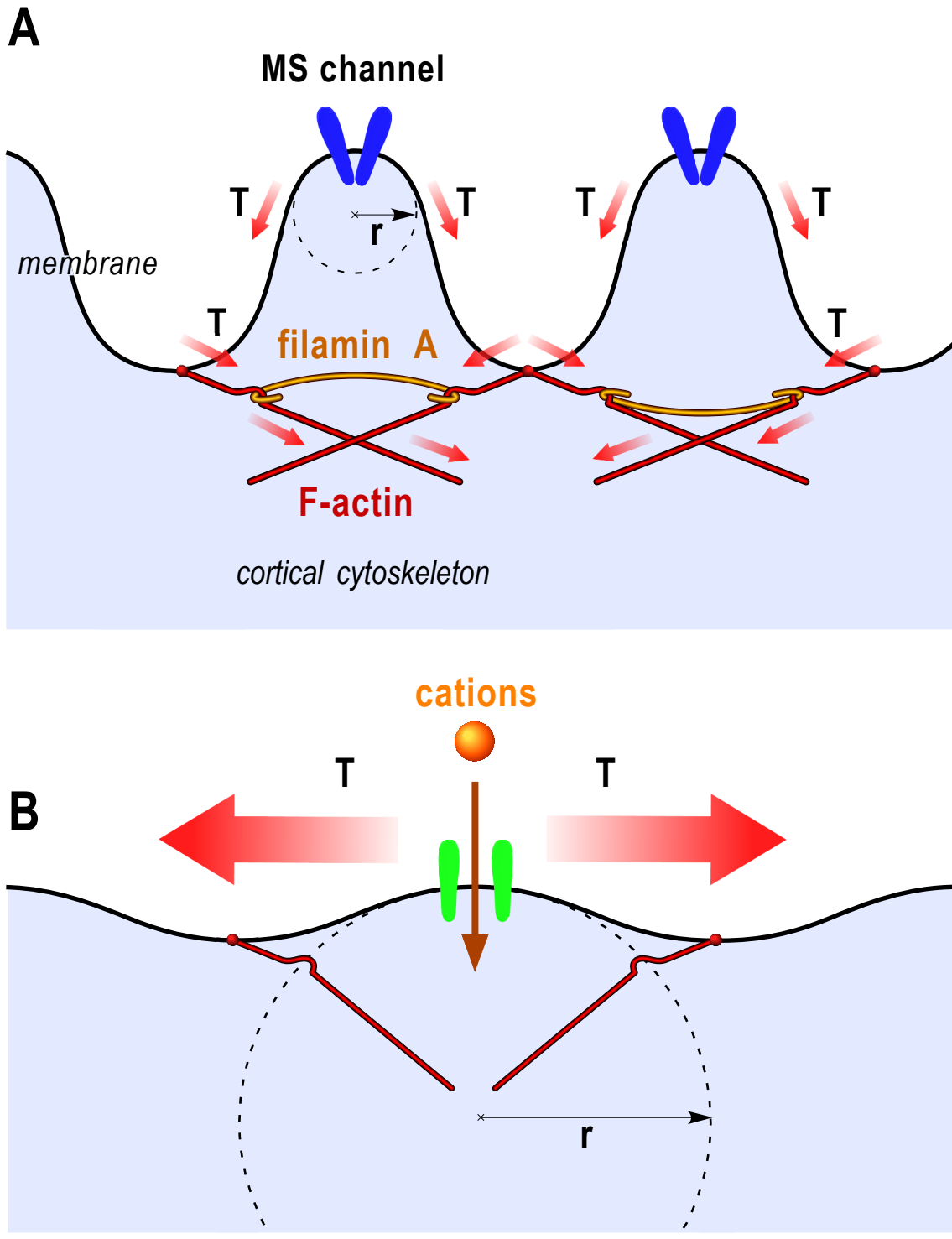
A
MS channel
T
T
r
T
T
membrane
T
filamin A
T
F-actin
cortical cytoskeleton
cations
B
T
T
r